

NONLINEAR MODEL PREDICTIVE CONTROL OF A SMART-SCALE EMULSION POLYMERIZATION PROCESS

Preet J. Joy¹, Adel Mhamdi¹, Falco C. Jung¹, Kristina Rossow², Hans-Ulrich Moritz², Werner Pauer² and Alexander Mitsos ^{*1}

¹Aachener Verfahrenstechnik - Process Systems Engineering (SVT), RWTH Aachen University, Turmstrasse 46, Aachen 52064, Germany

²Institute for Technical and Macromolecular Chemistry, University of Hamburg, Bundesstrasse 45, Hamburg 20146, Germany

Abstract

In this article a nonlinear model predictive control (NMPC) scheme for a smart-scale emulsion polymerization process is presented. The control objective is to maintain the product quality specifications and safe operating conditions even when the process is subject to disturbances or the product quality setpoint changes. The total monomer conversion and the polymer composition are used as a measure of product quality and the reactor temperature is used as a measure of process safety. The model is a set of differential algebraic equations, which captures the polymerization kinetics, mass transfer and heat transfer in the reactor as well as the dynamics of the auxiliary equipment - namely thermostats, pumps and mixing chambers. An extended Kalman filter is used to estimate unmeasured states, from measurements of temperature and mass of reactant fed to the reactor. The performance of the NMPC scheme is demonstrated in simulation case studies.

Keywords

Nonlinear model predictive control, state estimation, smart-scale reactor

Introduction

Emulsion polymerization is an industrially important process used to manufacture a variety of products like adhesives, paints, etc. (Asua, 2004). An alternative to conventional semi-batch reactors are the so-called smart-scale reactors (Lueth et al., 2013). These reactors are tubular reactors, which offer a high heat removal capacity, making them safer than semi-batch reactors. The control of such reactors, however, remains challenging due to tight product constraints, stringent environmental considerations and, temporal and spatial variation of process states.

There is limited work reported regarding model-based control of complex tubular processes, e.g., polymerization, which involve multiple phases and has coupled phenomena namely mass transfer, heat transfer

and chemical reactions. Vega et al. (1997) demonstrate in simulation and experiment the control of monomer conversion in a tubular solution polymerization reactor using a neural network model. Zavala and Biegler (2009) describe the implementation of a nonlinear model predictive control (NMPC) scheme for a tubular reactor manufacturing low-density polyethylene, where it is demonstrated that the controller is able to stabilize the reactor in the presence of fouling disturbances and profitability can be optimized using an economic objective. Gjertsen (2014) describes a simulation study of an NMPC implementation for a tubular emulsion polymerization reactor for handling setpoint changes for the monomer conversion and the reactor operating temperature.

In this work, we investigate the performance of an NMPC scheme for a complete tubular emulsion polymerization process, which includes a reactor and inter-

*To whom all correspondence should be addressed
Alexander.Mitsos@avt.rwth-aachen.de

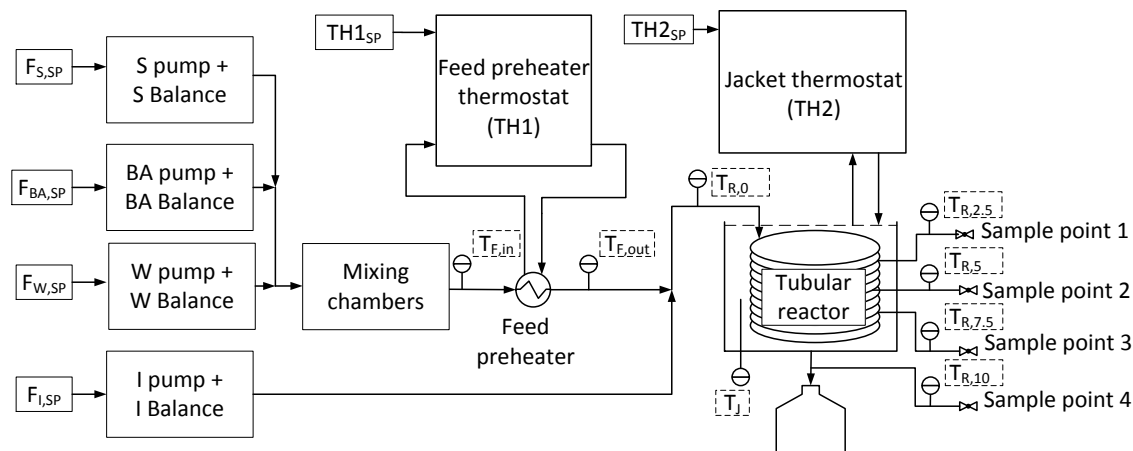


Figure 1. Flowsheet of the smart-scale emulsion polymerization process

acting auxiliary equipment. The main control objective is to ensure that requirements for product quality and safe operating conditions are met even if the process is subject to disturbances or the product specifications are changed.

Smart-scale Emulsion Polymerization Process

In Figure 1, a simplified flowsheet of the smart-scale emulsion polymerization process is shown. At the heart of the process is the tubular reactor (Rossow et al., 2016) immersed in an oil jacket. Diaphragm metering pumps are used to feed all streams into the reactor. The pump setpoints are $F_{S,SP}$, $F_{BA,SP}$, $F_{W,SP}$ and $F_{I,SP}$. The monomers (styrene - S, butyl acrylate - BA) are mixed with a water / emulsifier stream (W) in a sequence of two mixing chambers to ensure a well-mixed dispersion. This dispersion is heated in a feed preheater and mixed with the initiator stream (I) before entering the reactor. The feed preheater thermostat (TH1) helps to maintain a temperature at the reactor inlet high enough for the initiation of polymerization by the thermal decomposition of the initiator. The jacket thermostat (TH2) ensures that the reactor temperature is sufficient for a high monomer conversion. $TH1_{SP}$ and $TH2_{SP}$ are the setpoints to the jacket and the preheater thermostat, respectively. The reactor has temperature sensors located at the reactor inlet ($T_{R,0}$), at lengths 2.5 m ($T_{R,2.5}$), 5 m ($T_{R,5}$), 7.5 m ($T_{R,7.5}$) and reactor outlet ($T_{R,10}$). Sample points are also located at lengths 2.5 m, 5 m, 7.5 m and reactor outlet to collect samples for offline determination of conversion using gas chromatography. The

jacket is assumed to be well-mixed and its temperature (T_J) is also measured. Balances are used to record the mass of reagents fed to the reactor. The temperature and balance measurements are the only online measurements available.

Models of Different Process Components

In this section, we discuss briefly the models of the main process equipment.

Model of Tubular Reactor

The mechanistic model for the tubular reactor used is based on (Pokorny et al., 2016). It is also assumed that transfer to monomer does not take place and that the average number of radicals per particle is 0.5 (zero-one kinetics (Thickett and Gilbert, 2007)).

The first principles model of the tubular reactor results in a system of partial differential and algebraic equations (PDAEs) which are converted to a system of differential and algebraic equations (DAEs) using method of lines (MOL) (Schiesser, 1991). In this work, a discretization with 12 discretization points provides a satisfactory trade-off between computational demand and model accuracy. The model is implemented in the software gPROMS, has 110 differential equations, 1200 algebraic equations and requires 1.2 seconds to simulate 1 h of operation on a server running Intel Xeon, 2.6 GHz, 16 core processor with 96 GB RAM. For the parameter estimation of the reactor model, an identifiability analysis using the Eigenvalue method (Quaiser and Mönningmann, 2009) is carried out.

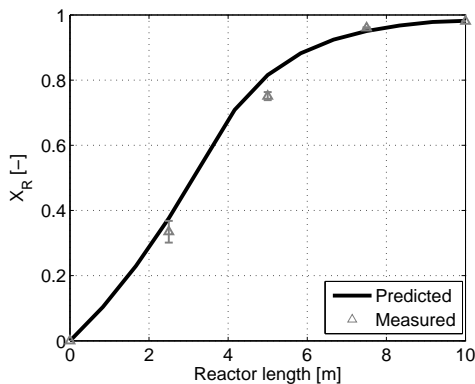


Figure 2. Comparison of measured and predicted values of total monomer conversion (X_R) at steady state

A set of 9 parameters, out of 23, were identifiable with steady state measurements of total and individual monomer conversion (obtained from offline GC measurements) as well as reactor temperature. For further details about experimental results from the smart-scale reactor refer to Rossow et al. (2016). During the parameter estimation, which was carried out in gPROMS, some of the identifiable parameters were observed to have large confidence intervals. These parameters were kept fixed at their literature values (taken from Pokorny et al. (2016)) and only those parameters which had an acceptable confidence interval were updated based on measurement data. The parameters that were adjusted are the rate coefficients for polymer propagation (2 parameters), the reactivity ratios (2 parameters) and the heat transfer coefficient. In Figure 2, we compare model prediction and measured values of total monomer conversion. Except for the measurement at 5 m, the model prediction is in good agreement with the observed measurements.

Models of Auxiliary Equipment

The model of the pumps comprise the calculation of the flow rates from the rate of change of balance measurements and a PI controller which adjusts the pump frequency to maintain the flow rates at the chosen setpoint. The mixing chambers also need to be modeled as they affect the time taken for change in concentration of monomers, due to a change in the pump flow rates, to be realized at the reactor inlet. The mixing chambers are modeled as perfectly mixed vessels.

Both the jacket and preheater thermostat have an oil bath, the temperature of which is maintained by adjusting the heating rate with the help of an internal PID

controller. The thermostats are assumed to have fixed cooling rates. The models for the jacket and preheater thermostat are developed by performing an energy balance of the streams entering and leaving the respective equipment.

State Estimation Using EKF

As the controlled variables (CVs), i.e., total monomer conversion and the polymer composition, are not measured online, they are estimated from the available measurements using an extended Kalman filter (Simon, 2006). A linear observability test for the tubular reactor reveals that the system is not observable but, detectable, which is required for stable estimation (Rawlings and Mayne, 2009).

The tuning parameters of the EKF are the matrices \mathbf{P}_0 (covariance of the initial state), \mathbf{Q} (covariance of the state noise) and \mathbf{R} (covariance of the measurement noise). To determine \mathbf{Q} , we use the approach suggested by Schneider and Georgakis (2013), i.e., $\mathbf{Q} = \mathbf{J}_{\hat{\mathbf{p}}} \cdot \mathbf{C}_{\hat{\mathbf{p}}} \cdot \mathbf{J}_{\hat{\mathbf{p}}}^T$, where $\mathbf{J}_{\hat{\mathbf{p}}} = \left. \frac{\partial \mathbf{f}}{\partial \hat{\mathbf{p}}} \right|_{ss}$ is the Jacobian of model equations w.r.t the estimated parameters $\hat{\mathbf{p}}$, evaluated at the steady state of the system. The matrix $\mathbf{C}_{\hat{\mathbf{p}}}$ is the covariance matrix of the estimated parameters $\hat{\mathbf{p}}$, which is obtained from gPROMS during parameter estimation.

NMPC Formulation

We use the NMPC formulation according to (Tiagounov and Weiland, 2003). Here the NMPC optimization problem is converted to a quadratic program wherein the future predictions are calculated as a combination of predictions using a nonlinear model with past inputs and prediction of future outputs using a linearized model defined along the predicted trajectory. The tuning of the NMPC is done to ensure that the setpoints of the CVs are satisfied and so that the manipulated variables have a smooth and non-oscillatory response.

Case Studies in Simulation

Simulation studies to test the NMPC are carried out using the OptoEcon toolbox (Elixmann et al., 2014). This toolbox allows for use of models implemented in a high-level modeling language like gPROMS. A model of the process is used as a plant replacement with no plant-model mismatch. Zero-mean Gaussian noises are added

to the outputs to simulate measurement errors. In all the simulation studies reported, a sampling time of 60 s is used. Two scenarios are considered for the testing of the NMPC scheme: (i) response to external disturbances and (ii) setpoint change for product quality.

Scenario I - Disturbance in Styrene Feed

A 40% step increase in the styrene flow rate serves as the disturbance in this scenario. The reactor temperature is used as a measure of process safety and is specified an upper bound of 110 °C. The CVs - the total monomer conversion and the styrene fraction in the polymer have setpoints 0.98 and 0.21, respectively. The manipulated variables (MV) are the butyl acrylate flow rate and the setpoints of the preheater and jacket thermostats.

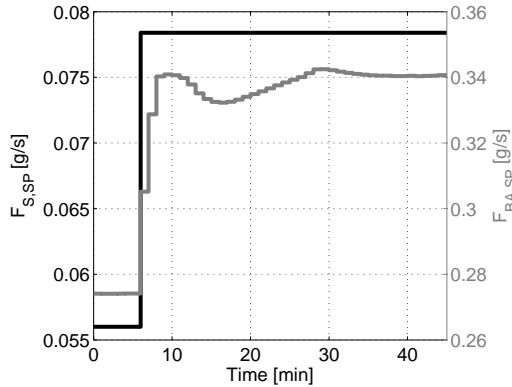


Figure 3. Monomer pump setpoints. $F_{S,SP}$ - assumed disturbance, $F_{BA,SP}$ - MV

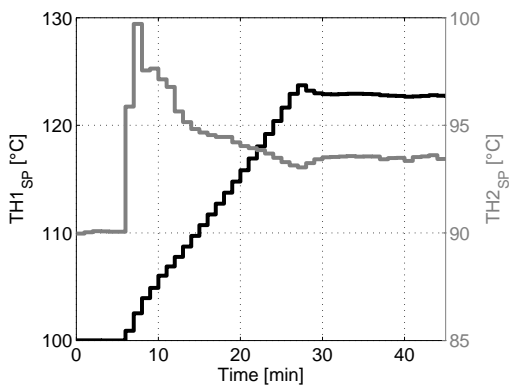


Figure 4. MVs - $TH1_{SP}$ and $TH2_{SP}$ in response to a disturbance

In Figure 3, we show the disturbance ($F_{S,SP}$) and the response of the NMPC on the BA pump ($F_{BA,SP}$). The NMPC adjusts the BA flow rate in order to maintain the final polymer composition.

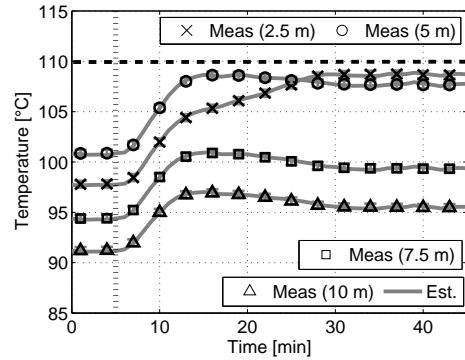


Figure 5. Temperature in the reactor

The NMPC action on the preheater and jacket thermostats is shown in Figure 4. Both the preheater and jacket thermostats are increased as a higher temperature is needed to achieve the specified conversion for an increased total monomer flow rate.

In Figure 5, we plot the temperature at the four measurement locations within the reactor. In general, an increase in temperature is observed due to a higher heat of reaction resulting from the additional monomer being fed to the reactor and due to the increased reactor inlet and jacket temperatures. The reactor temperature at 2.5 m which is lower than that at 5 m, is seen to increase more and become higher than the temperature at 5 m. This is due to the large increase in the reactor inlet temperature. The temperature at all the measurement points are kept below the specified constraint for the maximum reactor temperature.

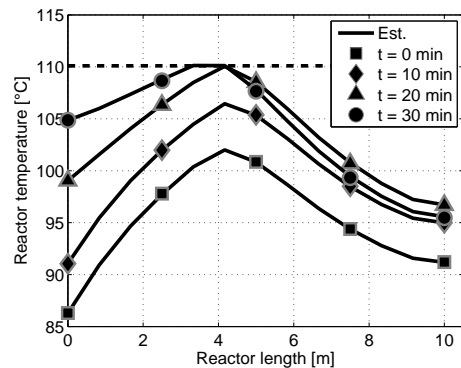


Figure 6. Evolution of temperature profile in the reactor

In Figure 6, we show the evolution of the temperature profile in the reactor at different time instances. Here we see that the maximum temperature in the reactor is at 4 m initially and as the reactor inlet temperature increases, the temperature in the first half (5 m) in the reactor increases significantly ~ 20 °C, while that in the second half of the reac-

tor increases to a smaller extent (7 - 8 °C). Note that at the final steady state the temperature within the reactor hits the upper bound between 2.5 and 5 m.

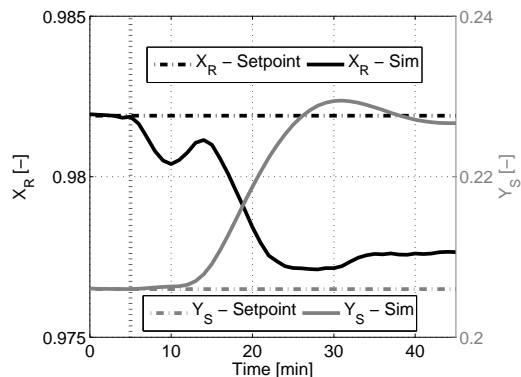


Figure 7. Total monomer conversion (X_R) and styrene fraction in polymer (Y_S) at reactor outlet in response to disturbance

The evolution of the CVs over the course of the NMPC simulation are shown in Figure 7. We observe that the total monomer conversion (X_R) decreases from its original value (prior disturbance) by $\sim 0.5\%$ and the polymer composition, represented in terms of the styrene fraction in polymer (Y_S), increases $\sim 2\%$. This deviation from the setpoint for the CVs is because the reactor temperature hits the specified constraint. In order to achieve the necessary conversion and composition a higher reactor temperature will be needed, which would be in violation of the specified safety constraints.

Scenario II - Change in Product Specification

In this scenario, the setpoint for the total monomer conversion is changed from 0.92 to 0.97 and the setpoint for the styrene fraction in the polymer is changed from 0.53 to 0.7. For this simulation study, the manipulated variables are the flow rate setpoint to the S and BA pumps, and the setpoints to the jacket and pre-heater thermostats. A maximum reactor temperature constraint of 105 °C is specified as a safety constraint.

In Figure 8, we see the response of the outlet reactor conversion and styrene fraction in the polymer to a setpoint change implemented at 8 min. Both the total monomer conversion (X_R) and the polymer composition (Y_S) attain their specified setpoint values. The delay in the response of the CVs to the change in the setpoint is due to the residence time of the reactor.

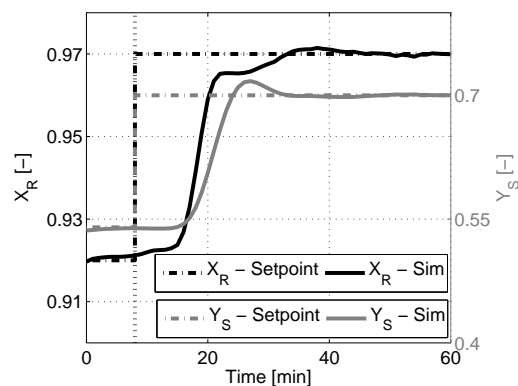


Figure 8. Total monomer conversion (X_R) and styrene fraction in polymer (Y_S) at reactor outlet in response to a setpoint change

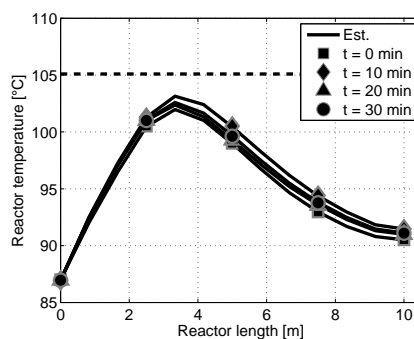


Figure 9. Evolution of temperature profiles at different time points

From Figure 9 we conclude that at all times the reactor temperatures are below the upper bound. Note that there is negligible change in the temperature profile.

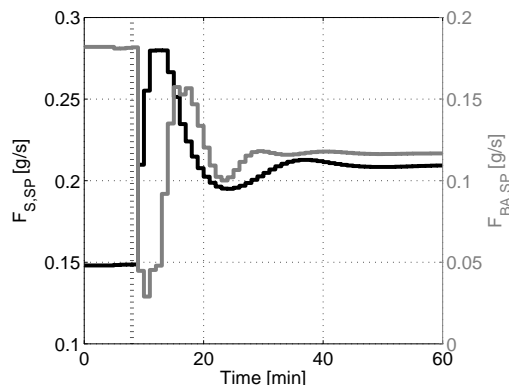


Figure 10. Response of the monomer pumps

In Figure 10 and Figure 11 the response of the manipulated variables in response to a setpoint change are shown. The monomer pumps are adjusted to attain the necessary composition at the exit. We observe that there is negligible change in the setpoints to the jacket and

preheater thermostats. Thus, the implemented NMPC scheme is able to successfully control the process for the considered setpoint change in the product quality.

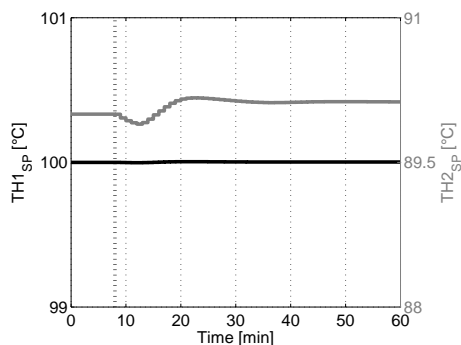


Figure 11. Response of preheater and jacket thermostats

Conclusions

In this work, the modeling and simulation results of an NMPC implementation of a smart-scale emulsion polymerization process are presented. When subject to external disturbances, the original monomer conversion and polymer composition were not met due to tight constraint on the reactor temperature. For a setpoint change in the product quality, the NMPC enabled a smooth transition from the first operating point to the second operating point.

For future work, the robustness to model error and the use of an economic MPC, instead of the setpoint tracking formulation, for the grade transitions may be investigated. The simulation results presented here is an intermediate step before experimental validation on the real smart-scale emulsion polymerization process.

Acknowledgments

This project has received funding from the European Union's Seventh Framework Program grant agreement no 280827 (COOPOL) and from the European Framework Horizon 2020, grant agreement no 636820 (RE-COBA).

References

- Asua, J. M. (2004). Emulsion polymerization: From fundamental mechanisms to process developments. *J. Polym. Sci. A Polym. Chem.*, 42:1025–1041.
- Elixmann, D., Puschke, J., Scheu, H., Schneider, R., Wolf, I. J., and Marquardt, W. (2014). A software environment for economic NMPC and dynamic real-time optimization of chemical processes. *at*, 62:150–161.
- Gjertsen, F. (2014). A modeling framework for control of smart-scale tubular polymerization reactors. Master's thesis, Norwegian University of Science and Technology (NTNU).
- Lueth, F. G., Pauer, W., and Moritz, H. U. (2013). Properties of smart-scaled PTFE-tubular reactors for continuous emulsion polymerization reactions. *Macromol. Symp.*, 333:69–79.
- Pokorný, R., Zubov, A., Matuška, P., Lueth, F., Pauer, W., Moritz, H. U., and Kosek, J. (2016). Process model for styrene and n-butyl acrylate emulsion copolymerization in smart-scale tubular reactor. *Ind. Eng. Chem. Res.*, 55:472–484.
- Quaiser, T. and Mönnigmann, M. (2009). Systematic identifiability testing for unambiguous mechanistic modeling - application to JAK-STAT, MAP kinase and NF-kappaB signaling pathway models. *BMC Syst. Biol.*, 3:50–71.
- Rawlings, J. B. and Mayne, D. Q. (2009). *Model Predictive Control: Theory and Design*. Nob Hill Publishing.
- Rossow, K., Broege, P., Lueth, F. G., Joy, P. J., Mhamdi, A., Mitsos, A., Moritz, H. U., and Pauer, W. (2016). Transfer of emulsion polymerization of styrene and n-butyl acrylate from semi-batch to a continuous tubular reactor. *Macromol. React. Eng.*, 10:324–338.
- Schiesser, W. E. (1991). *The Numerical Method of Lines: Integration of Partial Differential Equations*. Academic Press.
- Schneider, R. and Georgakis, C. (2013). How to not make the the extended Kalman filter fail. *Ind. Eng. Chem. Res.*, 52:3354–3362.
- Simon, D. (2006). *Optimal State Estimation*. John Wiley & Sons.
- Thickett, S. C. and Gilbert, R. G. (2007). Emulsion polymerization: State of the art in kinetics and mechanisms. *Polymer*, 48:6965–6991.
- Tiagounov, A. A. and Weiland, S. (2003). Model predictive control algorithm for nonlinear chemical processes. In *Proceedings of PHYSICON 2003*, volume 1-4, pages 334–339.
- Vega, M. P., Lima, E. L., and Pinto, J. C. (1997). Modeling and control of tubular solution polymerization reactors. *Comput. Chem. Eng.*, 21:S1049 – S1054.
- Zavala, V. M. and Biegler, L. T. (2009). Optimization-based strategies for the operation of low-density polyethylene tubular reactors: Nonlinear model predictive control. *Comput. Chem. Eng.*, 33:1735–1746.